

# Testing Transformer Learnability on the Arithmetic Sequence of Rooted Trees

Alessandro Breccia<sup>\*1</sup>, Federica Gerace<sup>1</sup>, Marco Lippi<sup>2</sup>, Gabriele Sicuro<sup>1</sup>, and  
Pierluigi Contucci<sup>1</sup>

<sup>1</sup>Department of Mathematics, University of Bologna, Italy

<sup>2</sup>Department of Information Engineering, University of Florence, Italy

December 2, 2025

## Abstract

We study whether a Large Language Model can learn the deterministic sequence of trees generated by the iterated prime factorization of the natural numbers. Each integer is mapped into a rooted planar tree and the resulting sequence  $\mathcal{NT}$  defines an arithmetic text with measurable statistical structure. A transformer network (the GPT-2 architecture) is trained from scratch on the first  $10^{11}$  elements to subsequently test its predictive ability under next-word and masked-word prediction tasks. Our results show that the model partially learns the internal grammar of  $\mathcal{NT}$ , capturing non-trivial regularities and correlations. This suggests that learnability may extend beyond empirical data to the very structure of arithmetic.

## 1 Introduction

Prime factorization, the decomposition of a natural number into its constituent primes, lies at the crossroads of arithmetic, complexity theory, and computational practice. While every integer admits a unique factorization, the operational effort required to obtain it grows quickly with its magnitude. State-of-the-art algorithms achieve remarkable performance for moderately large inputs, yet their complexity escalates rapidly when confronted with truly large instances. Moreover, in this limit, the sequence of integers with known prime factorizations becomes effectively sparse, with regions where the factorizations of intermediate values are computationally inaccessible.

It is therefore natural to ask whether modern machine learning methods, and more specifically Large Language Models (LLMs), can offer any advantages from this perspective.

---

<sup>\*</sup>alessandro.breccia2@unibo.it

In this work we start from the central observation that the sequence of prime factorizations, when iterated to the exponents, can be converted into an arithmetic text: each integer can be mapped to a rooted tree (see Eq. 1) encoding its multiplicative and exponential prime structure, or equivalently represented as a Dyck word, namely a balanced binary string. The resulting infinite sequence, denoted by  $\text{NT}$ , is a deterministic text, a symbolic unfolding where each structural “word” appears infinitely many times, much like recurring syntactic motifs in natural language that reemerge across different sentences.

In fact the statistical and some grammatical properties of  $\text{NT}$  have been studied in previous works, revealing a self-organized hierarchy of symbolic units, a sublinear growth of the dictionary, and long-range correlations that recall several features of natural languages (Contucci et al. 2025); (Conti and Contucci 2025); (Conti, Contucci, and Iudelevich 2024); (Conti, Contucci, and Iudelevich 2025). These observations suggest that the arithmetic text possesses an internal grammar, an emergent syntax rooted in the structure of the integers themselves.

Machine-learning approaches to arithmetic sequences have been investigated in numerous settings. Neural networks applied to the primes (He 2018) showed limited ability to reproduce their distribution, and theoretical arguments based on Kolmogorov-complexity (Kolpakov and Rocke 2023); (Kolpakov and Rocke 2024) suggest that the prime indicator function is not compressible within standard statistical frameworks. Related work on modular classification of integers (Jian Wu et al. 2023) shows that high accuracy is obtained only when externally provided arithmetic features are incorporated into the data representation.

Attempts to predict prime gaps or infer prime ratios using sequential or dense architectures (Pylov, Maitak, and Protodyakonov 2023); (Blake 2023) demonstrate local predictive ability over restricted ranges, but accuracy degrades as size increases and no structural inference emerges. Early neural factorization experiments (Jansen and Nakayama 2005) concluded that numerical encodings behave as noise beyond superficial correlations, and this has been confirmed with modern models (Nene and Uludag 2022), where degradation in performance with bit length strongly suggests that structural information is absent from raw inputs. More advanced diffusion-based refinement techniques (Freivalds, Ozoliņš, and Bārzdiņš 2023) have produced improved numerical results on limited ranges, but scaling issues remain.

Machine-learning methods have also been used to approximate the Möbius function and related arithmetic predicates (Qin and Ye 2024); (Lee and Kim 2024), often achieving high accuracy, but only when the input includes explicit structured information such as modular reductions or sparse encodings, indicating that the models exploit externally supplied arithmetic descriptors rather than discovering internal generative logic.

Most of these studies operate on representations that expose only partial aspects of the multiplicative structure of the integers, whether via numerical encoding, handcrafted features, or modular reductions. In the present work, the integers are represented through their complete multiplicative tree structure, encoded as Dyck words in the corpus  $\text{NT}$ .

The natural question that follows is whether this arithmetic language is also learnable. More precisely, *can LLMs exposed to the first portion of  $\mathbb{NT}$  infer the continuation of the sequence and fill in the gaps?* In this work we address this question by training a transformer-based network (the GPT-2 architecture, taken as canonical) on the sequence of Dyck words associated with the first few billions of integers. We consider two canonical self-supervised tasks, namely next word prediction (NWP) and masked language modelling (MLM), and we quantify the transformer’s performances on these two tasks both at the level of generic Dyck words and on specific ones of arithmetic interest, such as primes.

These experiments aim to shed light on two distinct yet complementary aspects: one primarily relevant to number theory and the other to machine learning. On one hand, they test whether a transformer can predict the prime factorization of an integer from the preceding ones and fill in the gaps in the sequence up to the first  $10^{11}$  integers. By comparing the transformer’s predictions with analytical and probabilistic baselines, we then assess the degree to which a neural architecture designed for human language can learn a deterministic arithmetic text. On the other hand, LLMs have shown remarkable ability to capture structure in human language, biological sequences, and symbolic domains such as mathematics. Yet, the emergence of this ability – namely the capacity to extract latent rules from raw sequences – remains mostly an empirical observation rather than a theoretically understood mechanism. To probe its foundations one may seek a language whose generative rule is known exactly. The infinite sequence of prime factorization  $\mathbb{NT}$  offers precisely such a testbed: because the data generating law is known, the problem becomes an experimental probe of learnability. We can indeed measure whether, how, and to what extent a model recovers the structure that produces the text.

Our study therefore lies at the intersection of mathematics, information theory, and machine learning, and provides preliminary evidence that transformers can learn text containing arithmetic information. Questions regarding their efficiency and how they compare to existing prime factorization algorithms are left for future investigation. The remainder of the paper introduces the dataset and notation (Section 2), describes the model architecture and training protocols (Section 3), and reports the experimental results for NWP and MLM together with baseline comparisons (Section 5).

## 2 Construction of the dataset

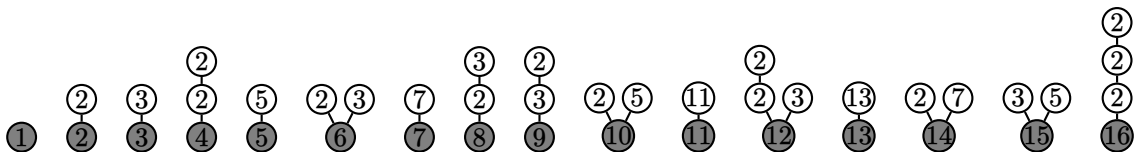
To produce our dataset, we proceed as follows. Let  $n \in \mathbb{N}$  be a natural number and  $\omega(n)$  the cardinality of the set of its prime factors. Let us consider the following representation  $\tau(n)$  of  $n$  (Conti and Contucci 2025):

- if  $n = 1$ , then  $\tau(n) = 1$ ;
- if  $n > 1$ , let  $n = \prod_{k=1}^{\omega(n)} p_k^{a_k}$  be its factorization in  $\omega(n)$  distinct primes,  $a_k \in \mathbb{N}$ , labeled in such a way that if  $k < k' \Rightarrow p_k < p_{k'}$ ; then  $\tau(n) = \{p_k : \tau(a_k)\}_{k=1}^{\omega(n)}$ .

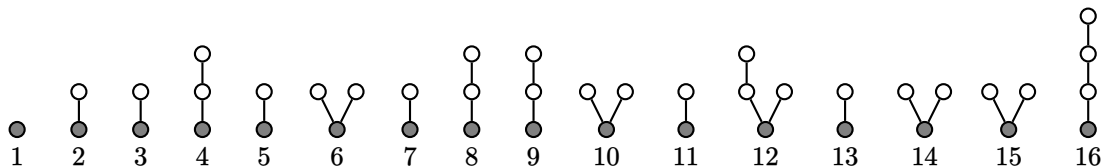
Such a representation of a natural number has been also analyzed by P. Devlin and Gnan (2014) — who called it *prime tower factorization* — and it is naturally associated to a tree (Childress 2021); (Iudelevich 2022), in which a root, associated to  $n$ , is linked to  $\omega(n)$  “parents”, each corresponding to one of its prime factors of  $n$ . Given the parent  $p_k$ , we iterate the construction associating to it  $\omega(a_k)$  parents, each for each prime factor of its exponent’s prime decomposition. The construction interrupts when a prime exponent equal to one appears. For example, for  $n = 55340232221128654848$ , we would naturally construct the representation

$$n = 2^{64} \cdot 3 = 2^{2^{2 \cdot 3}} \cdot 3 \mapsto \tau(n) = \{2 : \{2 : \{\{2 : 1\}, \{3 : 1\}\}\}, 3 : 1\} \mapsto$$
(1)

The natural numbers up to 16 can be represented as



We imagine that, at each generation, parents of a node are represented above it as nodes sorted in increasing order from left to right. The *depth* of a parent is the number of edges of the unique path joining it with the root along the tree. It is immediate to see that if  $n$  is prime,  $\tau(n) = \{n : 1\}$  and the corresponding tree consists of a dimer. If we focus on the *topology* of such trees, ignoring therefore the labels appearing in the nodes, the construction above associate to each natural number  $n > 1$  a rooted planar tree. As the emerging structure is undecorated, different number are mapped to the same tree topology, as it appears in the sequence below, where 6, 10, 14 and 15 are all mapped in the same “undecorated” rooted graph:



Some properties of the so-constructed sequence of trees have been investigated in the literature, for example with respect to their depth (De Koninck and Verreault 2024). On the other hand, each planar tree, can be represented as a Dyck path, or equivalently a binary string (Stanley 2011). Such a string, that we will denote by  $w(n)$  with respect to the natural number  $n$ , can be imagined as constructed starting from the root and moving

on the exterior of the tree from its leftmost edge: each time an edge is traveled upwards we insert a 1, each time an edge is traveled downwards we insert a 0. In the example above,  $n = 2^{2^2 \cdot 3} \cdot 3$  is therefore mapped into the string  $w(n) = 1110100010$ . As the tree exploration ends when we get back to the root, each of these binary representations contains necessarily as many 1s as 0s, always starting by 1 and ending by 0, in a way that on the left of each digit in the string there are no more 1s than 0s. In this representation, all prime numbers correspond to 10, as they are associated to the tree  $\textcircled{0}$ . Note that such a representation is obviously not in bijection with  $\mathbb{N}$ , nevertheless it contains information on the factorization properties of natural numbers (so that, for example 10 indicates that a number is prime, or a sequence  $1010 \dots 10$  of  $k$  repetitions of 10 express the fact that the number is a product of  $k$  distinct primes): as a result, the sequence of undecorated trees, that we denote  $\text{NT}$ , can be seen as a (lossy) translation of  $\mathbb{N}$  in a “language” of “Dyck words” following its own “grammatical rules” (Childress 2021). In fact, in a series of works (Conti and Contucci 2025); (Conti, Contucci, and Iudelevich 2024); (Conti, Contucci, and Iudelevich 2025), it was observed that the sequence  $\text{NT}$  exhibits a number of structural properties. Each Dyck word appears in the sequence, and it does so infinitely many times. Both properties are a direct consequence of the infinitude of prime numbers, and imply that the set  $\text{ND}$  of distinct Dyck words appearing in the sequence — the *dictionary* — is countably infinite. Certain phrases (finite sequences of Dyck words) occur only once, such as 10 10 or 1100 10, while others recur extremely often. For instance, the infinite occurrence of 10 1100 is equivalent to the still-open Mersenne conjecture; the infinite recurrence of 1010 10 relates to the Sophie Germain conjecture; and 1100 1100 is known to occur infinitely often, a fact established in 2004 with the proof of Catalan’s conjecture by Mihăilescu (2004). The text is moreover oriented: if one takes a valid phrase and reverses the order of its words, the resulting string is often invalid, i.e., it never occurs. For example, 111000 10 occurs many times, whereas 10 111000 can be proven never to appear. Further examples of impossible configurations of words include, as it is easy to prove, four consecutive square free numbers.

Our dataset consists of such a string representation for the first  $10^{11}$  natural numbers: as detailed in Section 5, the obtained structured sequence of strings has been fed to an LLM as though it were a long text, with the goal in mind of testing its predictive ability after learning. In the following, we will denote by  $\text{NT}_n$  the ordered sequence of undecorated trees corresponding to the first  $n$  natural numbers larger than 1 (so that  $|\text{NT}_n| = n - 1$ ). Similarly, we denote by  $\text{ND}_n$  the set of distinct trees appearing in  $\text{NT}_n$ , namely the dictionary required to write down  $\text{NT}_n$ . The statistical features of the database have been analyzed in (Contucci et al. 2025). That study provides some evidence that the arithmetic structure underlying the Natural text corpus produces an organized and self-consistent symbolic sequence. The number  $|\text{ND}_n|$  of distinct symbolic units grows sublinearly with  $n$ , indicating the emergence of internal grammatical rules and recursive patterns. The sequence is inherently oriented, with directionality embedded in its syntax, and shows a balance between redundancy and novelty as revealed by entropy and compression analyses. The rank–frequency hierarchy remains nearly invariant across scales, while correlation

studies expose long-range dependencies and a transition from diffusive to ballistic regimes. These resemblances with natural languages naturally lead to the question of whether, how, and to what extent the Natural text can be learned by a Large Language Model, the central question addressed in this paper.

### 3 Learning Model

*Transformers* (Vaswani et al. 2017) are a powerful type of neural network that is currently achieving state-of-the-art results in various domains, such as natural language processing (NLP) (J. Devlin et al. 2019); (Howard and Ruder 2018); (Radford, Narasimhan, et al. 2018); (Brown et al. 2020); (OpenAI 2024), image classification (Dosovitskiy et al. 2021), protein structure prediction (Jumper, Evans, et al. 2021) and detection of ground states of many-body quantum systems (Viteritti, Rende, and Becca 2023); (Rende, Viteritti, et al. 2023); (Viteritti, Rende, Parola, et al. 2023). Contrary to previous models of neural networks, transformers have been shown to be more adequate in capturing long-range correlations in sequential type of data, like, for instance, words in a sentence.

To learn these correlations, transformers rely on the so-called *self-attention mechanism*, which, roughly speaking, effectively transforms each element, or *word*,  $w_i$  within a “sentence”  $\mathbf{w} = (w_k)_{k=1}^L$  of length  $L$ , into another vector  $\mathbf{h}_i \in \mathbb{R}^d$ , where  $d \in \mathbb{N}$  is a hyper-parameter of the architecture<sup>1</sup>. Fig. 1 (left) illustrates the mechanism of self-attention using NLP as an explanatory example. Each word  $w_i$  is first mapped into a machine-readable, one-hot encoded vector  $\hat{\mathbf{t}}_i \in \mathbb{R}^d$  and then mapped, through an embedding matrix, into a  $d$ -dimensional vector  $\mathbf{t}_i \in \mathbb{R}^d$  named *token*. This continuous embedding space is essential for enabling self-attention to generalize across related symbols rather than treat each token as an unrelated categorical label (Mikolov et al. 2013). The self-attention layer then transforms each token  $\mathbf{t}_i$  into the vector  $\mathbf{h}_i$  as a linear combination of all the other tokens in the sentence, weighted by an attention matrix  $\mathbf{A} \in \mathbb{R}^{L \times L}$ , whose elements  $A_{ij}$  describe how relevant a token  $\mathbf{t}_j$  is to understanding the semantic meaning of token  $\mathbf{t}_i$ :

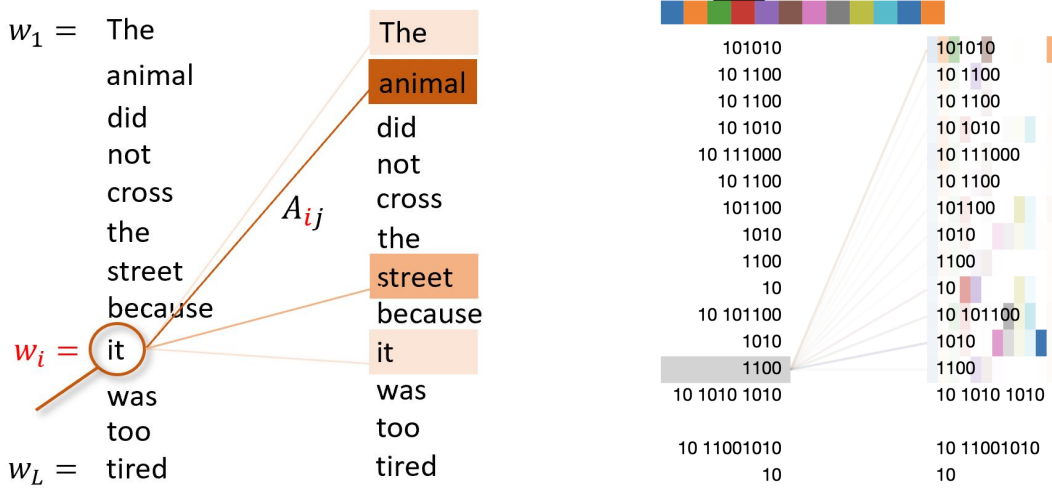
$$\mathbf{h}_i := \sum_{j \in [L] \setminus \{i\}} A_{ij} \mathbf{V} \mathbf{t}_j. \quad (2)$$

This sum is parameterized by a matrix  $\mathbf{V} \in \mathbb{R}^{d \times d}$  that is learned during training. The linear projection  $\mathbf{v}_i := \mathbf{V} \mathbf{t}_i$  is called *value*. The attention weights are computed by estimating a similarity score between the  $i$ -th token and all the other tokens in the sequence:

$$A_{ij} := \text{softmax} \left( \frac{\mathbf{t}_i^\top \mathbf{Q}^\top \mathbf{K} \mathbf{t}_j}{\sqrt{d}} \right) \quad (3)$$

---

<sup>1</sup>In general and in our setup the correspondence between words and tokens is not one-to-one, nevertheless we assume such a correspondence here for the sake of simplicity, delaying the details about the tokenization later in the text.



$$w_i \xrightarrow{\text{tokenizer}} t_i \xrightarrow{\text{attention}} h_i = \sum_{j \neq i} A_{ij} \mathbf{V} t_j, \quad \text{where} \quad A_{ij} = \text{softmax} \left( \frac{t_i^T \mathbf{Q}^T \mathbf{K} t_j}{\sqrt{d}} \right).$$

Figure 1: On the left, attention map at single layer level for a single head attention in an NLP setting: color represent the intensity of the attention value produced on the sentence words by focusing on word it. On the right, attention map for a multi-head attention in our setting corresponding to the ‘word’ 1100 highlighted in gray. In particular, on the right column each element of the arithmetic sequence is associated to a vector of colorbars, each representing a different head attention: the intensity of the color is proportional to the attention weight produced by the corresponding attention head.

where the two matrices  $\mathbf{Q} \in \mathbb{R}^{R \times d}$  and  $\mathbf{K} \in \mathbb{R}^{R \times d}$  are also learned: the dimension  $R$  is another hyperparameter of the system. The linear projections  $\mathbf{q}_i := \mathbf{Q} t_i$  and  $\mathbf{k}_i := \mathbf{K} t_i$  are called *query* and *key*, respectively. The terminology comes from databases, where to retrieve a value, we issue a query that is compared with all the keys in the database, and then select the value linked to the key most similar to the query.

The self-attention layers are typically pretrained via self-supervised tasks, that is tasks where the label is a part of the input itself. Some examples are *Masked Language Modelling* (MLM) or *Next-Word Prediction* (NWP). In the first case, the Transformer is trained to identify missing words within a text. In the second, it is tasked with predicting the next word in a sentence, given its preceding context. The quantity  $\mathbf{p}_\theta := \text{softmax}(\mathbf{h}_i)$  with  $\theta = \{\mathbf{Q}, \mathbf{K}, \mathbf{V}\}$  then represents a probability distribution across the sequence of tokens. For instance, it has been shown that, when trained via MLM, transformers learn the conditional distribution of a token given the surrounding context (Rende, Gerace, et al. 2024a); (Rende, Gerace, et al. 2024b). In the case of causal-attention for NWP, implemented to model



causally sequential data (as text), the lower triangular part of the attention matrix is set to  $-\infty$  before the softmax step. In such a way, tokens can only look for correlations with previous ones. By doing so, the model selectively aggregates information based on context, learning representations that are independent of the tokens positions. Therefore, positional embeddings are added to the tokens embedding to characterize the local information of data, that is not captured by attention on its own. Multi-head attention extends the aforementioned computations to a multiple, parallel version of self-attention layers, in which each head should ideally capture different patterns and relationships between tokens, allowing for more complex representations. A complete Transformer block is thus composed of a multi-head self-attention layer, a layer normalization regularizer and a feed-forward layer (Vaswani et al. 2017). Current models stack sequentially several of these blocks to create more refined and rich representations.

MLM and NWP are the two tasks on which we will test the ability of a Transformer to learn the internal grammar of  $\text{NT}$ : we will train it to both fill the gaps in the ensemble of currently known factorization of prime numbers, as well as to predict factorization of very large numbers. In the next section, we define more in detail these two tasks.

## 4 Tasks

We trained our LLM architecture focusing on two specific tasks. In both cases, the main goal is to evaluate whether and how much the architecture is able to learn the syntactical rules underlying the sequence  $\text{NT}$ . As anticipated, our base dataset consists of the ordered sequence of the first  $n$  trees  $\text{NT}_n$ , represented via Dyck words. This dataset is pre-processed and converted in a different dataset  $\bar{\mathcal{T}}_n$  via a *tokenizer* (see below): our architecture will be fed the sequences in the tokenized representation  $\bar{\mathcal{T}}_n$ . Let  $\bar{\mathcal{T}}_{\text{train}} \subset \bar{\mathcal{T}}_n$  be a collection of sequences of  $L$  consecutive tokens to be used for training, and  $\mathbf{t} = (\mathbf{t}_i)_{i=1}^L \in \bar{\mathcal{T}}_{\text{train}}$  a sequence of tokens associated to a sentence of the arithmetic text  $\text{NT}$  via a tokenizer. Similarly, let  $\bar{\mathcal{T}}_{\text{test}} \subset \bar{\mathcal{T}}_n$  be a collection of sequences of  $L$  consecutive tokens to be used for testing, such that  $\bar{\mathcal{T}}_{\text{test}} \cap \bar{\mathcal{T}}_{\text{train}} = \emptyset$ . The precise characterization of the training and test datasets will be given in Section 5. The goal of the training phase is then to find a configuration of the attention weights and values, that achieve optimal generalization performance on sentences the model has never seen during the training phase. The performance after training is estimated by some metric  $A(\mathbf{t})$  applied on an LLM-generated sequence of token  $\mathbf{t}$ , averaged over the test set  $\bar{\mathcal{T}}_{\text{test}}$ , namely

$$\bar{A} := \frac{1}{|\bar{\mathcal{T}}_{\text{test}}|} \sum_{\mathbf{t} \in \bar{\mathcal{T}}_{\text{test}}} A(\mathbf{t}). \quad (4)$$

We will specify below the specific form of  $A(\mathbf{t})$  adopted in our experiments.



**Next-Word Prediction.** Let us consider the sentence  $\mathbf{t} = (\mathbf{t}_i)_{i=1}^L \in \bar{\mathcal{T}}_{\text{train}}$  in the training dataset, and let  $\mathbf{t}_{1:k} := (\mathbf{t}_i)_{i=1}^k$  the sub-sentence consisting of the first  $k - 1$  words. In a Next-Word Prediction (NWP) task we train the same transformer architecture as above via gradient descent to predict the next token  $\mathbf{t}_L$  of the sequence, using cross entropy loss:

$$\mathcal{L}_n(\boldsymbol{\theta}) := -\frac{1}{|\bar{\mathcal{T}}_{\text{train}}|} \sum_{\mathbf{t} \in \bar{\mathcal{T}}_{\text{train}}} \frac{1}{L-1} \sum_{i=2}^L \ln p_{\boldsymbol{\theta}}(\mathbf{t}_i | \mathbf{t}_{1:i-1}) \quad (5)$$

in which  $p_{\boldsymbol{\theta}}(\mathbf{t}_i | \mathbf{t}_{0:i-1}) \in [0, 1]$  again represents the transformer’s output probability for the correct next token  $\mathbf{t}_i$  given the previous  $i - 1$  tokens, that is, the vector  $\mathbf{t}_{1:i-1}$ . Such a probability depends on the vector of parameters  $\boldsymbol{\theta} \in \mathbb{R}^P$  required by the architecture and is expressed and is obtained by applying the softmax activation function to the pre-activation of the last layer  $\mathbf{h} \equiv \mathbf{h}(\mathbf{t}_{1:i-1}) \in \mathbb{R}^D$  depending on the input sequence  $\mathbf{t}_{1:i-1}$ , so that the predicted probability distribution for the value of  $\mathbf{t}_i$ .

$$p_{\boldsymbol{\theta}}(\mathbf{t}_a | \mathbf{t}_{1:i-1}) := \frac{\exp(h_a/T)}{\sum_{k=1}^D \exp(h_k/T)}, \quad a \in [D]. \quad (6)$$

In the expression above, a *temperature* parameter  $T$  appears: its value is very relevant in the final performance of the LLM.

**Masked Language Modeling.** Given a subset  $\{\mathbf{t}_a\}_{a \in \mathcal{I}(\mathbf{t})}$  of tokens in  $\mathbf{t}$ , let  $\mathcal{I}(\mathbf{t}) \subset [L]$  be an index set, consisting of non-repeated randomly selected indices, representing 15% of the original sequence, that will identify the subset of “masked tokens”. Each masked element  $\mathbf{t}_a$ ,  $a \in \mathcal{I}(\mathbf{t})$ , is then randomly assigned to a given mask-element that can be the mask token  $\mathbf{M}$  with probability 75%, a different token randomly drawn from the dictionary with probability 15%, or it can remain unchanged with probability 10%. In a MLM task, we train a transformer via gradient descent to predict the possibly missing token  $\mathbf{t}_a$ ,  $a \in \mathcal{I}(\mathbf{t})$ , given the altered sequence  $\mathbf{t}_{\mathcal{Q}}$  obtained from  $\mathbf{t}$  by the described masking procedure on the token  $\mathbf{t}_a$ . This is achieved by minimizing on  $\mathbf{t}$  the cross-entropy loss

$$\mathcal{L}_m(\boldsymbol{\theta}) := -\frac{1}{|\bar{\mathcal{T}}_{\text{train}}|} \sum_{\mathbf{t} \in \bar{\mathcal{T}}_{\text{train}}} \frac{1}{|\mathcal{I}(\mathbf{t})|} \sum_{a \in \mathcal{I}(\mathbf{t})} \ln p_{\boldsymbol{\theta}}(\mathbf{t}_a | \mathbf{t}_{\mathcal{Q}}) \quad (7)$$

where the role of “true label” is taken, for each  $a$ , by the missing token  $\mathbf{t}_a$  itself, while  $p_{\boldsymbol{\theta}}(\mathbf{t}_a | \mathbf{t}_{\mathcal{Q}}) \in [0, 1]$  represents the transformer’s output probability about the true, missing token given all the others in the sentence that represent the context. This quantity depends on the vector of parameters  $\boldsymbol{\theta} \in \mathbb{R}^P$  in the architecture. Each output probability  $p_{\boldsymbol{\theta}}(\cdot | \mathbf{t}_{\mathcal{Q}})$  is obtained by applying the softmax activation function to the pre-activation of the last layer  $\mathbf{h} \equiv \mathbf{h}(\mathbf{t}_{\mathcal{Q}}) \in \mathbb{R}^D$  depending on the input masked sentence  $\mathbf{t}_{\mathcal{Q}}$  in the very same form as in Eq. (6).

## 5 Experiments

We conducted an extensive experimental evaluation to test the performance of the model described in Section 3 on two distinct training strategies, namely the next-word prediction task and the masked language modeling. To this end, we employed the large (ordered) dataset  $\text{NT}_n$  described in Section 2 that consists of the sequence of Dyck words that represent all the integer numbers from 2 up to  $n = 10^{11}$ . Such a dataset has been pre-processed via a tokenizer to produce a new representation  $\bar{\mathcal{T}}_n$  in terms of tokens.

**Data.** The ordered dataset  $\text{NT}_n$  was split into 10 chunks. Each one of the first 9 chunks was further split into the initial 75%,  $\text{NT}_n^{(k,\text{train})}$ , and the remaining 25%,  $\text{NT}_n^{(k,\text{vt})}$ , the former being added to the training set and the latter to the validation set (for  $k = 1, \dots, 9$ ) or to the test set (for  $k = 10$ ). So that finally  $\text{NT}_n = \bigoplus_{k=1}^{10} \left( \text{NT}_n^{(k,\text{train})} \oplus \text{NT}_n^{(k,\text{vt})} \right)$ , where by  $\oplus$  we denote the concatenation. With this splitting strategy, the validation set is more consistent with the training set in terms of statistical properties, thus representing a more robust evaluation set for the hyper-parameter selection phase. The set  $\text{NT}_n^{(10,\text{vt})}$  is, conversely, a piece of  $\text{NT}$  beyond the training and validation sets: it can have slightly different statistical properties with respect to the previous sequences, but it offers a very interesting benchmark to verify the accuracy of the model in predicting unseen intervals at arbitrary distance from our training dataset. The set  $\text{NT}_n^{(10,\text{vt})}$  is left for test purposes. As a result, the training set is  $\text{NT}_n^{\text{train}} := \bigoplus_{k=1}^{10} \text{NT}_n^{(k,\text{train})}$  and the validation set is  $\text{NT}_n^{\text{val}} := \bigoplus_{k=1}^9 \text{NT}_n^{(k,\text{vt})}$ . The processing of the dataset took place after a *tokenization* pre-processing procedure, which we describe in the next paragraph.

**Tokenization.** A widely adopted solution to transform text into a machine-readable format is the so-called *sub-words tokenization*. This strategy introduces an intermediate symbolic layer by segmenting text into sub-word units, enhancing the expressivity of the character based tokenization and optimizing the large dictionary of word-based encoding.

Let us suppose we are given a “sentence”, namely an ordered sequence of words  $\mathbf{w} = (w_1, w_2, \dots, w_\ell)$  of length  $\ell$ . This sequence is represented as a sequence of characters from the finite and fixed text alphabet  $\mathcal{A} := \{0, 1, \_ \}$  consisting of 0, 1 and spaces, namely  $x_i \in \mathcal{A}$  for all  $i$ . The tokenization  $\mathbf{t}$  produces a new string of length  $\hat{\ell}$ , in general different from  $\ell$ , in the form

$$\mathbf{w} = (w_1, w_2, \dots, w_\ell) \mapsto \mathbf{t}(\mathbf{w}) = (\mathbf{t}_1, \mathbf{t}_2, \dots, \mathbf{t}_{\hat{\ell}}).$$

Each token  $\mathbf{t}_a \in \mathbb{R}^d$  appearing in  $\mathbf{t}(\mathbf{w}) = (\mathbf{t}_a)_{a=1}^{\hat{\ell}}$  is a  $d$ -dimensional vector in the tokenizer dictionary  $\mathcal{D}$ : the size  $|\mathcal{D}|$  of the tokenizer dictionary and the dimension  $d$  of the embedding space are tunable hyperparameters: in our experiments we considered  $D \in \{64, 256, 1024\}$ . Moreover, we selected  $d = 12 \times 64$  as we adopted a 12-heads GPT2 architecture, requiring

dimension 64 for each head (see below). Note that the original dictionary (namely, the number of different Dyck words appearing in our training dataset) is  $|\text{ND}_{9 \cdot 10^{10}}| > 2000$ . In our experiments, the Byte-Pair Encoding (BPE) algorithm (Sennrich, Haddow, and Birch 2016) has been used to construct the aforementioned dictionary, via the following scheme: given an initial dictionary  $\mathcal{D} = \mathcal{A}$  made of all characters, at each iteration  $k$ , the algorithm computes the frequency  $f_k(\mathbf{a}, \mathbf{b})$  of all adjacent symbol pairs  $(\mathbf{a}, \mathbf{b}) \in \mathcal{D} \times \mathcal{D}$  occurring in the corpus. Then, the pair with the highest frequency

$$(\mathbf{a}^*, \mathbf{b}^*) = \arg \max_{(\mathbf{a}, \mathbf{b})} f_k(\mathbf{a}, \mathbf{b})$$

is replaced with a new, single character associated with a new vector  $\mathbf{t}_{\text{new}} \in \mathbb{R}^d$ . The vocabulary  $\mathcal{D}$  is updated as  $\mathcal{D} \mapsto \mathcal{D} \cup \{\mathbf{t}_{\text{new}}\}$ . This process is iterated until the desired tokenizer dictionary size  $D := |\mathcal{D}|$  is reached. This tokenization ensures lossless encoding/decoding and high compression thanks to the hierarchical, frequency-based structure. By applying such tokenizer on the set  $\text{NT}_n^{(\text{train})}$ , we obtain a sequence of tokens that is further split in consecutive “sentences” of length  $L = 1024$ : we obtained, in this way, a tokenized dataset of sentences  $\tilde{\mathcal{T}}_{\text{train}}$ . Similarly, the test set  $\tilde{\mathcal{T}}_{\text{test}}$  is obtained by tokenizing  $\text{NT}_n^{(10, \text{vt})}$  and then sampling  $m$  sequences of sentences of length  $L$ . The sentence length  $L$  has been kept fixed for all runs of the experiments.

**Architecture.** The model used in our work is a *transformer decoder*, inspired by the OpenAI GPT-2 architecture (Radford, Jeffrey Wu, et al. 2019). It consists of 12 layers, each combining sequentially multi-head attention, layer normalization and finally a feed-forward neural network. A single head has dimension 64, and since the multi-head attention is composed of 12 heads, this leads to an embedding dimension  $d = 768$ , as anticipated. The GeLU activation function has been used as nonlinear activation. The resulting architecture has  $P = 8.7 \cdot 10^7$  trainable parameters.

## 5.1 A baseline: a Markov chain approach

As a first minimal baseline for our prediction tasks we considered a simple Markov chain (MC) (Kemeny and Snell 1983), that can be considered a minimal, almost memory-less model to predict a sequence. Let  $D$  be the size of the tokenizer dictionary, as before. Supposing the dictionary elements to be labeled as  $\mathcal{D} = \{\mathbf{t}_i\}_{i=1}^D$ , the chain simply consists of a transition matrix  $\Phi = (\Phi_{ij})_{ij} \in \mathbb{R}^{D \times D}$  such that  $\Phi_{ij}$  expresses the probability of observing the  $i$ th immediately after the  $j$ th token. The  $D(D-1)$  free parameters of  $\Phi$  have been determined by using ADAM optimizer on the empirical average negative log-likelihood, computed on the very same dataset used for the LLM training. The performance of the Markov chain will be used as minimal baseline for our results, as we expect our LLM to be *at least* as good as a vanilla Markovian model.

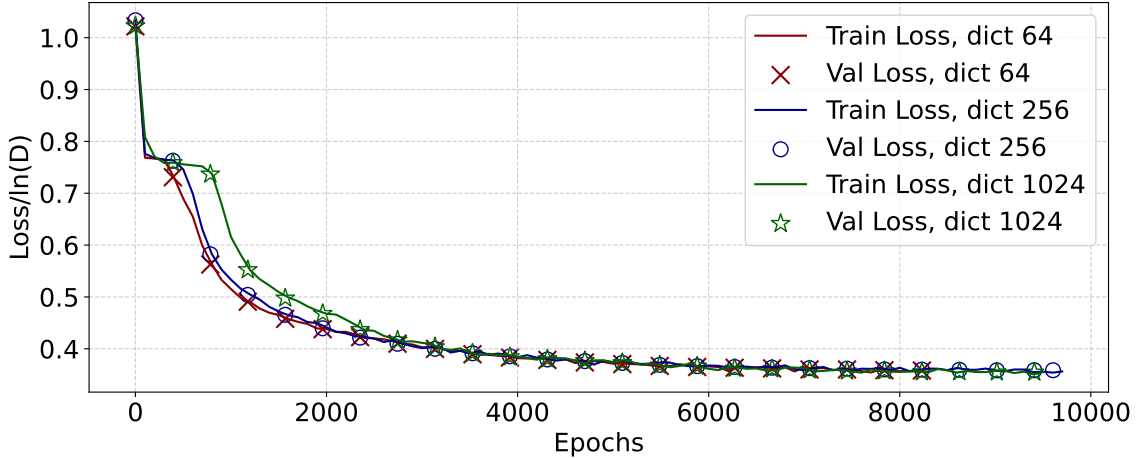


Figure 2: Loss curves for a model trained via NWP, obtained for different tokenizer’s dictionary size  $D$ , namely  $D = 64$ ,  $D = 256$ ,  $D = 1024$ . The loss value is rescaled by  $\ln D$ , loss value associated to a uniform distribution.

## 5.2 Next-Word Prediction

Let us start by presenting the performance of the model trained on the task Next-Word Prediction. The prompt is constructed with a context of  $L = 1024$  tokens, with no further instruction. The LLM then generates the continuation of the sequence. As customary with neural architectures (Bengio 2012), the training phase exploits an early stopping procedure on the loss computed over the validation set, with a patience value equal to 6 (i.e., training continues until the validation loss sees no improvement for 6 consecutive epochs). As for the evaluation phase, we sample  $m$  different sequences of 1024 tokens from the test set, and we feed them as prompts, letting the LLM generate another 1024 tokens. The generation process strongly depends on the temperature hyperparameter  $T$  appearing in Eq. (6), which controls the smoothness of the probability distribution over the tokens: low values of  $T$  sharpen the probability distribution, by concentrating the probability mass on the most likely outcomes only (with  $T \rightarrow 0$  a deterministic last-layer behaviour is obtained); high temperature values instead flatten the distribution, thus increasing the probability of less likely tokens (as  $T \rightarrow \infty$  assigns the same probability to all the tokens).

Figure 2 reports the learning curves for this task, namely the training and validation losses with three different tokenizer’s vocabulary sizes  $D$  (64, 256, and 1024 tokens, respectively), rescaled by  $\ln D$ , value of the loss on the uniform distribution over all the dictionary entries (or, equivalently, the  $T \rightarrow \infty$  case). After an initial rapid decrease, all three curves show an interesting brief initial plateau phase, which anticipates a second descent and appears to extend further in training as  $D$  increases: this behavior, to be further investigated in future research, suggests that the model might first initially discover

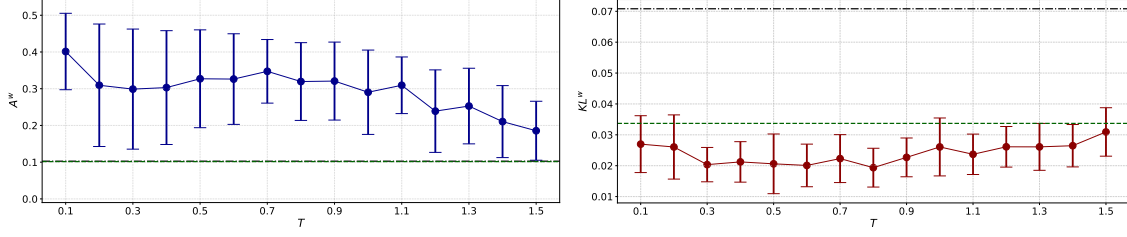


Figure 3: Accuracy for words ( $A^w$ , left) and Kullback-Leibler divergence for word distribution ( $KL^w$ , right) are reported at different temperature values  $T$ , averaged over a set of 32 different inputs for each  $T$ . The green dotted line represents the Markov Chain (MC) model baseline, while the black dash-dotted line identifies the large temperature limit.

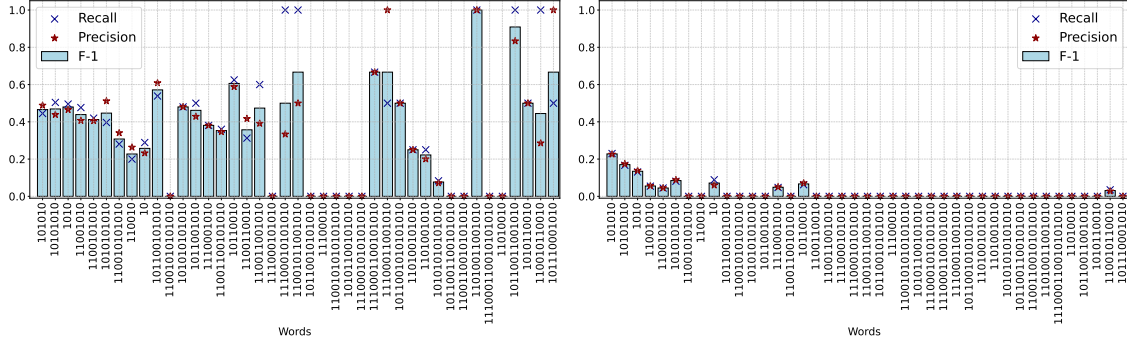


Figure 4: Precision, recall and  $F_1$  score for a set of  $L = 1024$  generated tokens. The  $x$ -axis is ordered by words' frequencies in the input sentences, namely the true sequence. On the left, result for our LLM model; on the right, corresponding quantities for the Markov baseline.

some basic properties of the sequence, while learning only in a second phase more complex relations (Rende, Gerace, et al. 2024a); (Cagnetta et al. 2025).

In order to measure the performance of the model, we considered several metrics  $A$  in the test error introduced in Eq. (4). The metrics compare an LLM-generated token sequence  $\mathbf{t} = (t_a)_{a=1}^L$ , with the associated reconstructed Dyck word sequence  $\mathbf{w}(\mathbf{t}) = (w_a(\mathbf{t}))_{a=1}^\ell$ , with the true ordered Dyck word sequence  $\hat{\mathbf{w}} = (\hat{w}_a)_{a=1}^\ell$  appearing in the true sequence, with respect to the same location<sup>2</sup>. First, we considered the *word accuracy*

$$A(\mathbf{t}) \mapsto A^w(\mathbf{t}) := \frac{1}{\ell} \sum_{a=1}^{\ell} \mathbb{I}(w_a(\mathbf{t}) = \hat{w}_a),$$

<sup>2</sup>It is not *a priori* obvious that the token sequence corresponds to a legit Dyck word sequence, e.g., in principle Dyck words like 1101 might appear when tokens are replaced with the corresponding character sequence: nevertheless we observed that our LLM almost never produced such illegal Dyck words.

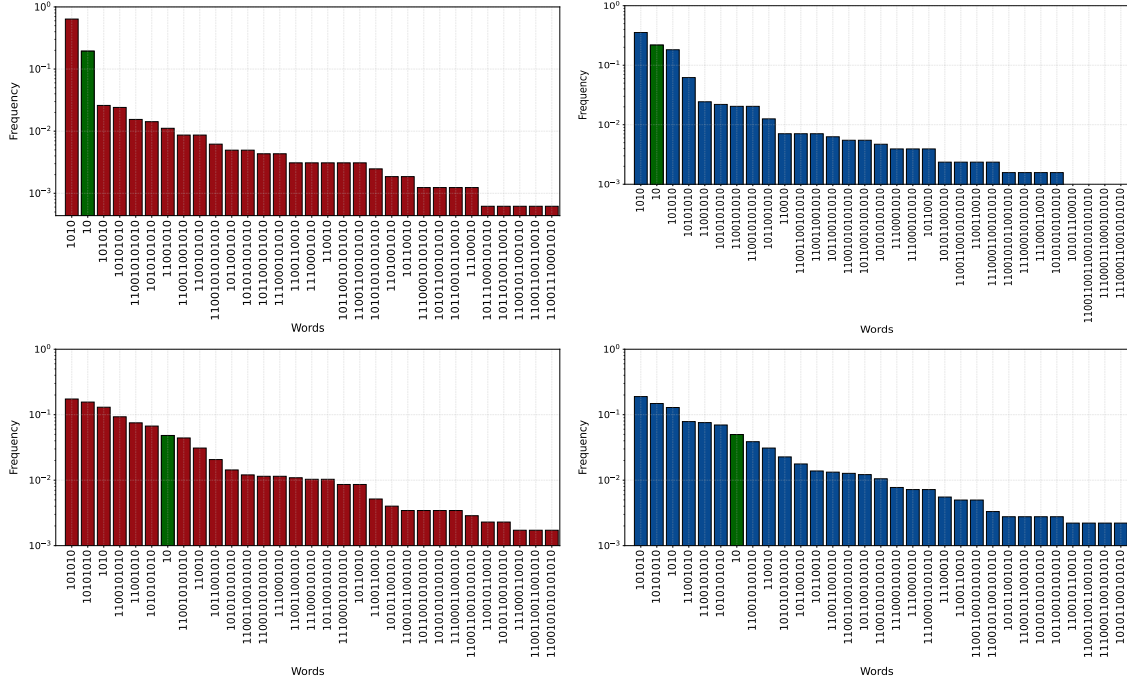


Figure 5: Distributions of the generated Dyck words at real prime positions (left) and of real words at predicted prime positions (right), averaged over a set of 10 generations of 1024 tokens. The LLM output (top row) is compared with a simple Markov model prediction (bottom row), showing better performances in both cases. Bars with label the string 10 correspond to correct predictions.

accuracy at the level of words, i.e., the number of correctly predicted Dyck words within a given sequence. We also adopted the metric

$$A(\mathbf{t}) \mapsto \text{KL}^w(\mathbf{t}) := \sum_w f_w(\hat{\mathbf{w}}) \ln \frac{f_w(\hat{\mathbf{w}})}{f_w(\mathbf{w}(\mathbf{t}))}.$$

In the expression above,  $f_w(\mathbf{w})$  is the empirical frequency of the word  $w$  in the sentence  $\mathbf{w}$ , the sum running on all distinct words in  $\mathbf{w}(\mathbf{t})$ , so that  $\text{KL}^w(\mathbf{t})$  is the Kullback–Leibler divergence between the empirical frequencies of Dyck words computed from the true and predicted sequences, respectively. In Figure 3 we report the values of  $\overline{A}^w$  and  $\overline{\text{KL}}^w$ , obtained by averaging over the test set the metrics above, as a function of the hyperparameter  $T$ . The results clearly show that our model largely outperforms the Markov chain baseline described above (red dotted line) whose performance has been quantified by means of the same quantities. The plots also highlight how performance degrades when  $T > 1$ , which is not surprising. The best results in terms of  $\overline{A}^w$  are obtained at low values of  $T$ , in the range

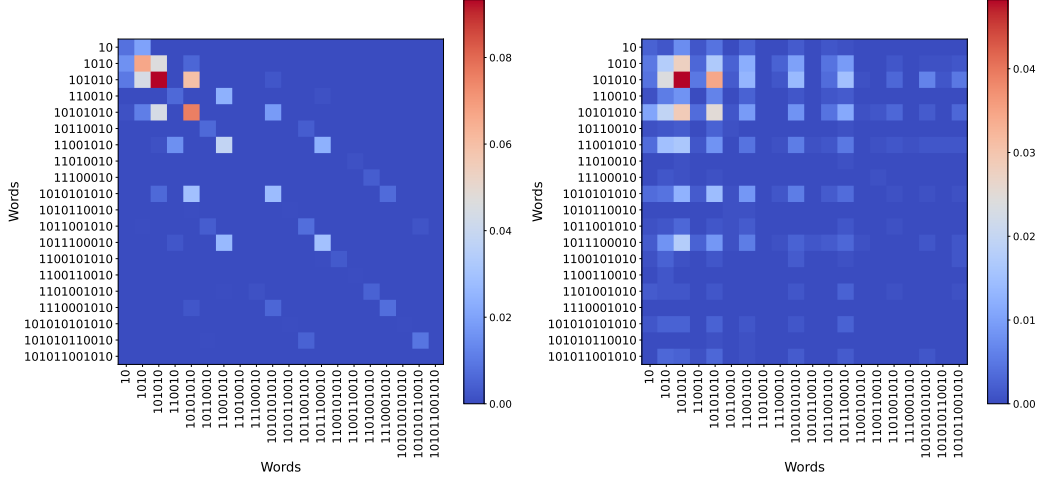


Figure 6: Confusion matrix for next word prediction task for the LLM (left) and the Markov model (right), normalized by the total number of words.

$0.1 \leq T \leq 0.3$ , while  $\overline{\text{KL}}^w$  has its best value for  $0.3 \leq T \leq 0.7$ . This likely happens because the value of the word accuracy  $\overline{A}^w$  is dominated by high-frequency words, i.e., the correct detection of the words that appear most frequently induces a high value of accuracy.

The aforementioned two metrics are global metrics that do not consider how accurate is the model in predicting rare Dyck words, and in particular prime numbers, which we are clearly very interested in predicting correctly. Specifically, just by accurately predicting the most frequent words in the sequence, a high value can be obtained for  $\overline{A}^w$  and a low value for  $\overline{\text{KL}}^w$ . For this reason, we also considered the *precision*  $P^w(\mathbf{w})$ , the *recall*  $R^w(\mathbf{w})$ , and the *score*  $F_1^w(\mathbf{w})$  in the prediction  $\mathbf{w} = (w_a)_{a=1}^\ell$  of an  $\ell$ -words sentence corresponding to the ground truth  $\hat{\mathbf{w}} = (\hat{w}_a)_{a=1}^\ell$ . Intuitively, the precision  $P^w(\mathbf{w})$  is defined as the fraction of correctly predicted words of type  $w$  in the sentence  $\mathbf{w}$  over all predicted  $w$ -words, whereas the recall  $R^w(\mathbf{w})$  is the fraction of words of type  $w$  in the true sequence that are correctly detected. More precisely, we can define as False Positives  $\text{FP}_w(\mathbf{w}) := \sum_i \mathbb{I}(w = w_i) \mathbb{I}(w \neq \hat{w}_i)$  the number of predicted  $w$ -words within the sequence  $\mathbf{w}$  that are actually misclassifications of other words, whereas False Negatives  $\text{FN}_w(\mathbf{w}) := \sum_i \mathbb{I}(w \neq w_i) \mathbb{I}(w = \hat{w}_i)$  are missed  $w$ -words. The number of True Positives  $\text{TP}_w(\mathbf{w}) := \sum_i \mathbb{I}(w = w_i) \mathbb{I}(w = \hat{w}_i)$  counts those  $w$ -words that are correctly identified within the given sequence  $\mathbf{w}$ . Then, we have for a given sequence  $\mathbf{w}$

$$P^w(\mathbf{w}) := \frac{\text{TP}_w(\mathbf{w})}{\text{TP}_w(\mathbf{w}) + \text{FP}_w(\mathbf{w})} \quad , \quad R^w(\mathbf{w}) := \frac{\text{TP}_w(\mathbf{w})}{\text{TP}_w(\mathbf{w}) + \text{FN}_w(\mathbf{w})} \quad (8a)$$



whereas  $F_1^w(\mathbf{w})$  is the harmonic mean between precision and recall

$$F_1^w(\mathbf{w}) := 2 \left( \frac{1}{P^w(\mathbf{w})} + \frac{1}{R^w(\mathbf{w})} \right)^{-1}. \quad (8b)$$

In the case where  $w = 10$  we obtain precision, recall and  $F_1$  score for prime numbers. We remark that *both* precision *and* recall are very important to measure, since a recall equal to 1 could trivially be obtained by always predicting a prime, whereas a high precision could be achieved by seldom predicting a prime, only when the model has a very high confidence. Note that precision, recall, and  $F_1$  score can be computed also for all the other words, as if they were specific classes of a plain classification task. In Figure 4 we present the investigation of these metrics by reporting the values of precision  $P^w$ , recall  $R^w$ , and the  $F_1^w$  score for each word in the dictionary. For example, the metrics obtained for the word 10 are precision, recall and  $F_1$  score associated with prime numbers: we can observe that the three metrics are all close to 0.3, indicating that our model correctly detects one prime number roughly every three *existing* primes, as well as correctly predicts one prime number every three *predicted* primes. For other words, such as some square free integers (e.g., 1010, 101010, 10101010, etc.) the reported metrics are even higher, around 0.4–0.5.

To better analyze the errors made by the LLM in relation to prime numbers, we report in Fig. 5 the distributions of generated words in appearing in position occupied by primes in the true sequence (i.e., false negatives conditioned on primes) and that of words appearing in the true sequence when the LLM predicts a prime (i.e., false positive conditioned on primes). Interestingly, we notice how the model very frequently confuses primes with square free numbers. This behavior is confirmed also by the whole confusion matrix, which we report in Fig. 6.

### 5.3 Masked Language Modelling

Let us now briefly discuss the results obtained for the second considered training task, namely masked word prediction. As anticipated, here the goal is to predict missing tokens within a sequence that have been *masked*, i.e., removed at inference time. A crucial, additional hyper-parameter of this experiment is clearly the percentage of tokens that have been masked, which we name  $p_m$ . Similarly to the NWP task case, in Fig. 7 we report the learning curves for two different vocabulary sizes ( $D = 64$  and  $D = 256$  tokens, respectively). In this task, the initial plateau phase appearing in the NWP case is even more evident and extends further as  $D$  increases.

As in the NWP case, the output probability distribution is given in the form in Eq. (6) and depends therefore on the hyperparameter  $T$ . We analyzed the joint impact of the temperature  $T$  and the masking probability  $p_m$  in Fig. 8. Here we plot the performance of the model in the form of Eq. (4) by adopting a *token accuracy*,

$$A(\mathbf{t}) \mapsto A^t(\mathbf{t}) := \frac{1}{L} \sum_{a=1}^L \mathbb{I}(\mathbf{t}_a = \hat{\mathbf{t}}_a),$$

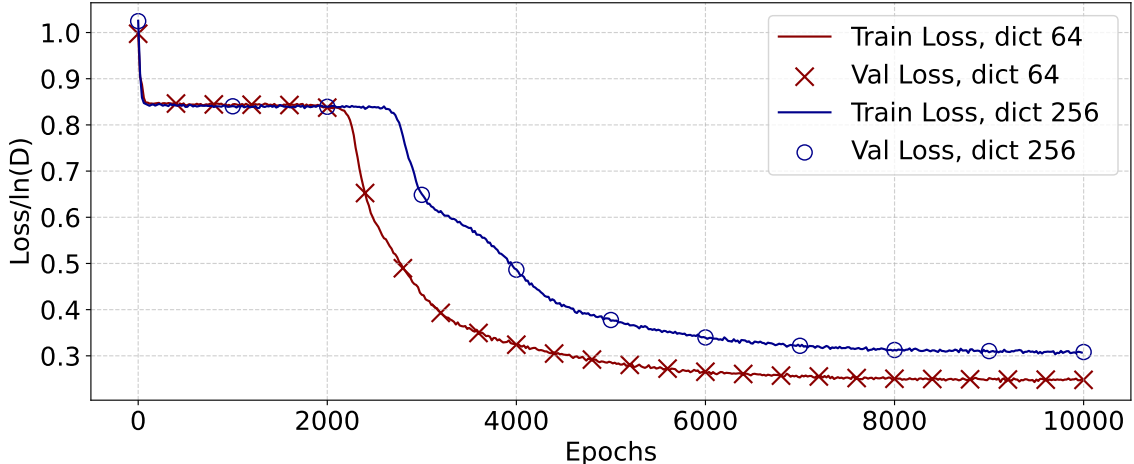


Figure 7: Loss curves for an architecture trained via masked language modelling. Here it is adopted a tokenizer dictionary size equal to  $D = 64$  and  $D = 256$ . The loss value is rescaled by  $\ln D$ , loss value associated to a uniform distribution.

namely an accuracy measure on the token sequence that compares a generated sequence  $\mathbf{t} = (t_a)_{a=1}^L$  with the corresponding true token sequence  $\hat{\mathbf{t}} = (\hat{t}_a)_{a=1}^L$  obtaining by tokenizing the ground truth word succession. A clear pattern appears indicating that performance degrades when both  $p_m$  and  $T$  grow, which is of course not surprising. Within the low temperature regime (in the range  $0.1 \leq T \leq 0.3$ ), the accuracy on tokens is above 0.4, remaining above 0.3 even with values of  $p_m$  and  $T$  growing up to 0.4 and 0.5, respectively.

## 6 Conclusions and Future Work

The results of this study suggests that a transformer network can partially infer the internal syntax of a deterministic arithmetic text when integers are represented through their rooted-tree structure. This observation hints that the “language of numbers” possesses a genuine “grammar” that can be approximated but not yet fully captured by the adopted architecture. The distinction between statistical correlation and structural dependence emerges clearly: arithmetic relations require context-sensitive reasoning rather than frequency-based learning.

Even a compact model such as GPT-2 is able to achieve measurable success in predicting classes of arithmetic interest such as primes and square-free numbers. The next step is to extend this experiment to larger-scale language models, endowed with wider context windows and richer embedding spaces, to test whether long-range dependencies and hierarchical relations among integers can be reconstructed. In fact, the limitations observed in the model’s predictions should be read as a reflection of its representational boundary.

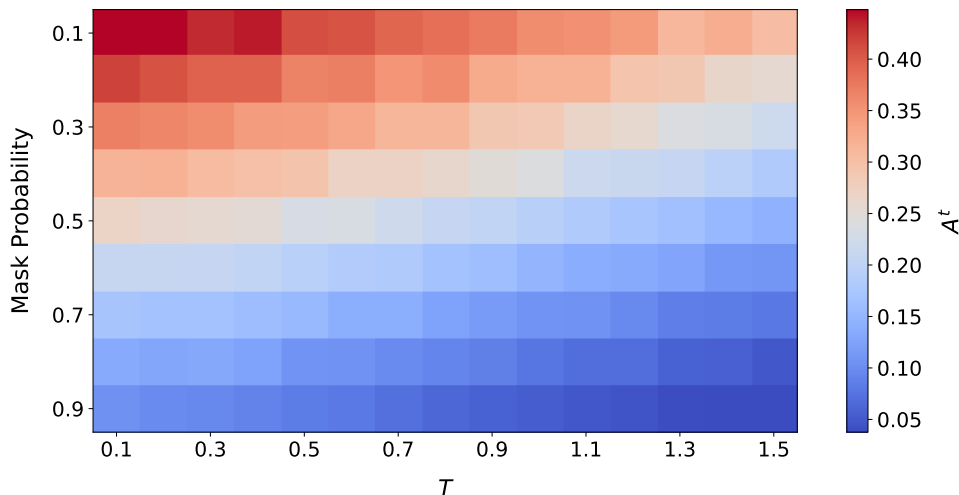


Figure 8: Tokens accuracy as function of masking probability and temperature  $T$  within the Masked Language Modelling strategy.

Within the horizon of its context window, GPT-2 learns all that can be learned from local multiplicative correlations, reproducing the “grammar of factorization” with remarkable internal consistency. Its errors arise precisely where the information required for prediction exceeds the model’s scope—at prime boundaries, where the continuation of the text is no longer determined by prior context. In this sense, the model predicts as far as its structure allows: it learns up to the limit of what can be inferred statistically from local dependencies. Beyond that limit, the sequence requires global reasoning and awareness of asymptotic density, features that lie outside the expressive reach of the architecture. The boundary of prediction thus becomes an experimental measure of the boundary of understanding.

Future work will focus on probing the internal representations of trained networks, to assess whether their latent spaces mirror algebraic proximity among numbers and encode a topology of multiplication. In this way, studying the learnability of arithmetic sequences may become a new empirical approach to understanding how structure gives rise to meaning — an experimental bridge between language models and number theory.

## Acknowledgments

The authors are grateful to Alina Sîrbu for providing the code to generate the database and Riccardo Rende for preliminary code and experiments on MLM. This research was performed under the auspices of Italian National Group of Mathematical Physics (GNFM) of the National Institute for Advanced Mathematics - INdAM. The authors acknowledge

the financial support from the European Union - Next Generation EU - Grant PRIN 2022B5LF52. This project received support from the EU H2020 ICT48 project Humane AI Net (grant no. 952026), the Italian Ministry of University and Research PRIN 2022 (code J53D23003690006), and the Italian Extended Partnership PE01—FAIR (Future Artificial Intelligence Research, proposal code PE000000013) under the National Recovery and Resilience Plan. Federica Gerace is supported by European Union-NextGenerationEU (NGEU) and she is partially supported by project SERICS (PE000000014) under the MUR National Recovery and Resilience Plan.

## References

- Bengio, Yoshua (2012). “Practical recommendations for gradient-based training of deep architectures”. In: *Neural networks: Tricks of the trade: Second edition*. Springer, pp. 437–478.
- Blake, Sam (2023). *Integer Factorisation, Fermat and Machine Learning on a Classical Computer*. arXiv: [2308.12290 \[cs.LG\]](#).
- Brown, Tom et al. (2020). “Language models are few-shot learners”. In: *Advances in neural information processing systems* 33, pp. 1877–1901.
- Cagnetta, Francesco et al. (2025). *Scaling Laws and Representation Learning in Simple Hierarchical Languages: Transformers vs. Convolutional Architectures*. arXiv: [2505.07070](#).
- Childress, Ralph L. (2021). “Recursive Prime Factorizations: Dyck Words as Numbers”. In: arXiv: [2102.02777 \[cs.FL\]](#).
- Conti, Roberto and Pierluigi Contucci (2025). “A Natural Avenue”. In: *Experimental Mathematics*, pp. 1–7.
- Conti, Roberto, Pierluigi Contucci, and Vitalii V. Iudelevich (2024). “Bounds on tree distribution in number theory”. In: *Annali dell’Università di Ferrara* 70 (3).
- (2025). *Tree Asymptotic Densities in Number Theory*.
- Contucci, Pierluigi et al. (2025). *Statistical Properties of the Rooted-Tree Encoding of  $\mathbb{N}$* . To appear in arXiv.
- De Koninck, Jean-Marie and William Verreault (2024). “On the Tower Factorization of Integers”. In: *The American Mathematical Monthly* 131.6, pp. 511–518. DOI: [10.1080/00029890.2024.2322912](#).
- Devlin, Jacob et al. (2019). *BERT: Pre-training of Deep Bidirectional Transformers for Language Understanding*. arXiv: [1810.04805](#).
- Devlin, Patrick and Edinah Gnang (2014). *Primes Appearing in Prime Tower Factorization*. arXiv: [1204.5251 \[math.NT\]](#).
- Dosovitskiy, Alexey et al. (2021). *An Image is Worth  $16 \times 16$  Words: Transformers for Image Recognition at Scale*. arXiv: [2010.11929 \[cs.CV\]](#).

- Freivalds, Kārlis, Emīls Ozoliņš, and Guntis Bārzdiņš (2023). “Discrete Denoising Diffusion Approach to Integer Factorization”. In: *Artificial Intelligence Applications and Innovations (AIAI 2023)*. Vol. 14272. Lecture Notes in Computer Science. Springer, pp. 123–134. DOI: [10.1007/978-3-031-44207-0\\_11](https://doi.org/10.1007/978-3-031-44207-0_11).
- He, Yang-Hui (2018). “Deep-Learning the Landscape”. In: *arXiv preprint*. arXiv: [1706.02714 \[hep-th\]](https://arxiv.org/abs/1706.02714).
- Howard, Jeremy and Sebastian Ruder (2018). *Universal Language Model Fine-tuning for Text Classification*. arXiv: [1801.06146 \[cs.CL\]](https://arxiv.org/abs/1801.06146).
- Iudelevich, Vitalii V. (2022). “On the “tree” structure of natural numbers”. In: *Discrete Mathematics and Applications* 32.5, pp. 325–340.
- Jansen, B. and K. Nakayama (2005). “Neural networks following a binary approach applied to the integer prime-factorization problem”. In: *Proceedings. 2005 IEEE International Joint Conference on Neural Networks, 2005*. Vol. 4, pp. 2577–2582.
- Jumper, John, Richard Evans, et al. (Aug. 2021). “Highly accurate protein structure prediction with AlphaFold”. In: *Nature* 596, pp. 1–11. DOI: [10.1038/s41586-021-03819-2](https://doi.org/10.1038/s41586-021-03819-2).
- Kemeny, John G. and J. Laurie Snell (1983). *Finite Markov Chains*. Undergraduate Texts in Mathematics. Springer New York. ISBN: 9780387901923.
- Kolpakov, Alexander and Aidan Rocke (2023). *On the Impossibility of Discovering a Formula for Primes Using AI*. arXiv: [2308.10817 \[cs.CC\]](https://arxiv.org/abs/2308.10817).
- (2024). *Machine Learning of the Prime Distribution*. arXiv: [2403.12588 \[cs.IT\]](https://arxiv.org/abs/2403.12588).
- Lee, Serin and S. Kim (2024). *Exploring Prime Number Classification: Achieving High Recall Rate and Rapid Convergence with Sparse Encoding*. arXiv: [2402.03363 \[math.NT\]](https://arxiv.org/abs/2402.03363).
- Mihăilescu, Preda (2004). “Primary cyclotomic units and a proof of Catalans conjecture”. In: *Journal für die reine und angewandte Mathematik* 2004.572, pp. 167–195.
- Mikolov, Tomas et al. (2013). *Efficient Estimation of Word Representations in Vector Space*. arXiv: [1301.3781 \[cs.CL\]](https://arxiv.org/abs/1301.3781). URL: <https://arxiv.org/abs/1301.3781>.
- Nene, Ryan and Suleyman Uludag (2022). “Machine Learning Approach to Integer Prime Factorisation”. In: *ResearchGate Preprint*. DOI: [10.13140/RG.2.2.25570.81602](https://doi.org/10.13140/RG.2.2.25570.81602).
- OpenAI (2024). *GPT-4 Technical Report*. arXiv: [2303.08774 \[cs.CL\]](https://arxiv.org/abs/2303.08774).
- Pylov, Petr, Roman Maitak, and Andrey Protodyakonov (2023). “Approximation Model Based on LSTM for Predicting the Next Prime Number in an Infinite Sequence”. In: *E3S Web of Conferences*. Vol. 413. EDP Sciences, p. 06009. DOI: [10.1051/e3sconf/202341306009](https://doi.org/10.1051/e3sconf/202341306009).
- Qin, Huan and Yangbo Ye (2024). “Algorithms of the Möbius Function by Random Forests and Neural Networks”. In: *Journal of Big Data* 11.31, pp. 1–16. DOI: [10.1186/s40537-024-00889-7](https://doi.org/10.1186/s40537-024-00889-7).
- Radford, Alec, Karthik Narasimhan, et al. (2018). *Improving language understanding by generative pre-training*.
- Radford, Alec, Jeffrey Wu, et al. (2019). “Language models are unsupervised multitask learners”. In: *OpenAI blog* 1.8, p. 9.

- Rende, Riccardo, Federica Gerace, et al. (2024a). “A distributional simplicity bias in the learning dynamics of transformers”. In: *Advances in Neural Information Processing Systems* 37, pp. 96207–96228.
- (2024b). “Mapping of attention mechanisms to a generalized potts model”. In: *Physical Review Research* 6.2, p. 023057.
- Rende, Riccardo, Luciano Loris Viteritti, et al. (2023). *A simple linear algebra identity to optimize Large-Scale Neural Network Quantum States*. arXiv: [2310.05715 \[cond-mat.str-el\]](#).
- Sennrich, Rico, Barry Haddow, and Alexandra Birch (2016). *Neural Machine Translation of Rare Words with Subword Units*. arXiv: [1508.07909 \[cs.CL\]](#).
- Stanley, Richard P. (2011). *Enumerative Combinatorics*. 2nd ed. Cambridge Studies in Advanced Mathematics. Cambridge University Press.
- Vaswani, Ashish et al. (2017). “Attention is all you need”. In: *Advances in neural information processing systems* 30.
- Viteritti, Luciano Loris, Riccardo Rende, and Federico Becca (June 2023). “Transformer Variational Wave Functions for Frustrated Quantum Spin Systems”. In: *Phys. Rev. Lett.* 130 (23), p. 236401. DOI: [10.1103/PhysRevLett.130.236401](#).
- Viteritti, Luciano Loris, Riccardo Rende, Alberto Parola, et al. (2023). *Transformer Wave Function for the Shastry-Sutherland Model: emergence of a Spin-Liquid Phase*. arXiv: [2311.16889 \[cond-mat.str-el\]](#).
- Wu, Jian et al. (2023). “Classification of Integers Based on Residue Classes via Modern Deep Learning Algorithms”. In: *Patterns* 4.9, p. 100860. DOI: [10.1016/j.patter.2023.100860](#).